Transactions of the VŠB – Technical University of Ostrava, Mechanical Series
No. 1, 2012, vol. LVIII
article No. 1904

Michal KOZDERA[*], Sylva DRÁBKOVÁ[**], Adam BUREČEK[***], Jaroslav KRUTIL[****]

REGIME OF THE FLOW IN THE AXIAL HYDROSTATIC BEARING WITH CENTRAL GROOVE

REŽIM PROUDĚNÍ V AXIÁLNÍM HYDROSTATICKÉM LOŽISKU S CENTRÁLNÍ DRÁŽKOU

Abstract

This paper deals with the fluid flow in the axial hydrostatic bearing with the central groove. The type of flow in the narrow gap is defined by the dimensionless Reynolds number. The influence of the groove shape on the pressure field in axial hydrostatic bearing is investigated. Numerical modelling and evaluation of the flow field parameters is done using Ansys Fluent software.

Abstrakt

Tento článek se zabývá prouděním kapaliny v axiálním hydrostatickém ložisku s centrální drážkou. Je definován typ proudění v úzké mezeře pomocí bezrozměrného Reynoldsova čísla. V práci je porovnán vliv tvaru drážky na tlakové pole v axiálním hydrostatickém ložisku. Výpočet a vyhodnocení parametrů proudového pole je provedeno pomocí programu Ansys Fluent.

1 INTRODUCTION

Axial hydrostatic bearings are basically simple devices. A layer of lubricant is fed between two planar surfaces, which transfer the load. These sliding bearings are used as rotary tables most often. In these devices the load is caused by the weight of the body, which is located on the bearing. They are used for example at machine tools for attaching the work piece or on large telescopes or cranes to perform the rotational movement of the device.

The advantage of axial hydrostatic bearings is very high load carrying capacity. They are suitable for all rotational speeds unlike the axial hydrodynamic bearings, which are not suitable for low speed of rotation. Axial hydrostatic bearings have infinite durability, which depends on the reliability of the external pressure source. Between the sliding pairs arises fluid friction and therefore they have very low frictional resistance. Their disadvantage is lower ability to absorb vibration and more demanding to operate than hydrodynamic bearings.

The lubricated fluid is supplied with the assistance of hydraulic aggregate. Load capacity of the axial hydrostatic bearing is then induced by hydrostatic pressures in the liquid, which generates hydraulic generator or more hydraulic generators at a time. Before entering into the bearing there is a throttle valve that regulates the flow rate, see Fig. 1. Bearing itself consists of two parts. The lower

[*] Ing. Michal KOZDERA, VŠB – Technical University of Ostrava, Faculty of Mechanical Engineering, Department of Hydromechanics and Hydraulic Equipment, 17. listopadu 15/2172, 708 33, Ostrava, Czech Republic, tel.: (+420) 59 732 4385, e-mail: m.kozdera@gmail.com

[**] doc. Ing. Sylva DRÁBKOVÁ, Ph.D., VŠB – Technical University of Ostrava, Faculty of Mechanical Engineering, Department of Hydromechanics and Hydraulic Equipment, 17. listopadu 15/2172, 708 33, Ostrava, Czech Republic, tel.: (+420) 59 732 4386, e-mail: sylva.drabkova@vsb.cz

[***] Ing. Adam BUREČEK, VŠB – Technical University of Ostrava, Faculty of Mechanical Engineering, Department of Hydromechanics and Hydraulic Equipment, 17. listopadu 15/2172, 708 33, Ostrava, Czech Republic, tel.: (+420) 59 732 4268, e-mail: adam.burecek@seznam.cz

[****] Ing. Jaroslav KRUTIL, VŠB – Technical University of Ostrava, Faculty of Mechanical Engineering, Department of Hydromechanics and Hydraulic Equipment, 17. listopadu 15/2172, 708 33, Ostrava, Czech Republic, tel.: (+420) 59 732 4270, e-mail: jkrutil@seznam.cz

part of the bearing is fixed with lubrication grooves on the sliding surface. The upper part has a smooth sliding surface and it can perform the movement. If the axial hydrostatic bearing is at rest, the upper part is lying on the lower part and the bearing does not move. When the lubricated liquid is brought into the grooves, the hydrostatic pressure starts to act on the upper part. When the upper part due to the fluid pressure lifts, a fluid layer is created and the bearing can move.

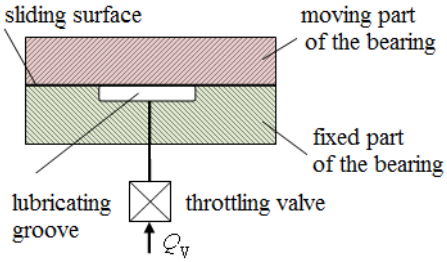

Fig. 1 Scheme of the axial hydrostatic bearing with central groove.

In the article, 3 types of axial hydrostatic bearings are compared. The individual variants differ among themselves in the shape of lubrication grooves, see Fig. 2. All three types consist of two plates which have a circular shape with the diameter of 500 mm. The mineral oil is brought into the inlet hole of the bearing with a diameter of 10 mm. There the liquid is distributed into the individual lubrication grooves. In all three variants the grooves were chosen so that the total area in the plan was the same. The depth of the grooves will be compared for 2 and 0.2 mm. Height of fluid layer between fixed and moving parts is 0.13 mm.

Variant a) it is assumed that incoming liquid will have the maximum pressure in the axis of axial hydrostatic bearing and the parabolic decrease towards the fluid outlet of the bearing can be expected. His large and substantial disadvantage is that it can be loaded only in the axis of bearing. For eccentric loads, the upper part is tilting and come into contact with the fixed part. This would cause friction change from liquid to dry and lead to wear surfaces. One of the possibilities is to design the bearings with multiple inputs evenly spaced across the surface. Then there is a need to connect the throttle valve to each input for regulation of the flow.

For variants b) and c) the shape of the grooves was designed which should prevent tilting of the upper part. In this case the application of bearings with multiple inputs has not to be used. For variant b) liquid is brought into a circular pocket and then into 4 rectangular grooves which spill liquid into 4 directions. For variant c) lubrication grooves are further branched in comparison with variant b).

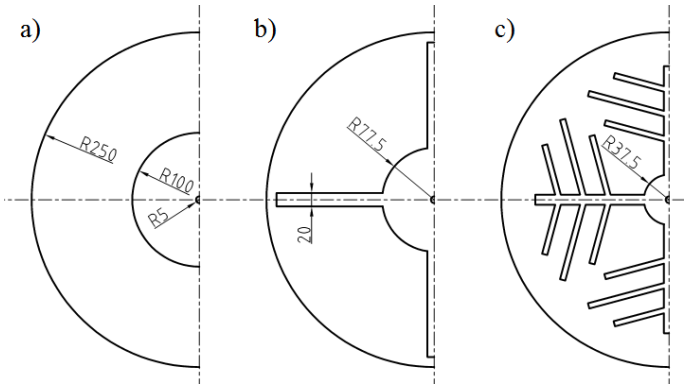

Fig. 2 Geometry of the axial hydrostatic bearing with central groove.

2 MATHEMATICAL MODEL OF THE AXIAL HYDROSTATIC BEARING WITH CENTRAL GROOVE

Since this is a narrow gap in the flow, where the size of fluid layer is 0.13 mm, it is assumed that the liquid will flow in very thin layers. Therefore, we assume laminar flow. Fluid flow is associated with the solution of the problem, which is defined as:

- three dimensional flow,
- incompressible flow (ρ = constant),
- laminar flow,
- isothermal flow (T = constant),
- stationary flow ($\partial / \partial t = 0$),
- flow without considering transmission additions.

Calculation and post processing of the results was performed using Ansys Fluent software. Prismatic grid with half a million cells was applied. At the inlet into the bearing the flow rate was set to 0.5 $dm^3.min^{-1}$. Mineral oil with a density 889 $kg.m^{-3}$ and viscosity 46 $mm^2.s^{-1}$ was defined.

2.1 Definition of regime of the flow

When defining the type of the flow, we use Reynolds number. The Reynolds number (Re) is a dimensionless number that gives a measure of the ratio of inertial forces to viscous forces. Turbulent vortices are characterized by length scale l $[m]$ and velocity scale u $[m.s^{-1}]$. These scales are called macro scales. Turbulent flow can also be characterized by the molecular properties represented by molecular viscosity ν $[m^2.s^{-1}]$. Using these variables, we can define Reynolds number

$$\mathrm{Re}_l = \frac{u \cdot l}{\nu}, \tag{1}$$

we can proceed with

$$\mathrm{Re}_l = \frac{u \cdot l}{\nu} \cdot \frac{l}{l} = \frac{\frac{l^2}{\nu}}{\frac{l}{u}} = \frac{T_\nu}{T_t}, \tag{2}$$

where:

T_ν is the time scale of molecular diffusion

T_t is the time scale of transport by turbulent eddies.

The flow can be characterized by Reynolds number as follows:

- $T_\nu \langle T_t$ i.e. $\mathrm{Re}_l \langle 1$: molecular diffusion processes dominate and termination of turbulent vortices can be expected. This type of flow is indicated as laminar.
- $T_\nu \rangle T_t$ i.e. $\mathrm{Re}_l \rangle 1$: turbulent vortices survive, inequality is true for relatively values of flow parameters. Most flows occurring in practice are turbulent.
- $T_\nu \rangle\rangle T_t$ i.e. $\mathrm{Re}_l \rangle\rangle 1$: viscous phenomena that effect the time scale can be neglected due to the dynamics of vortices. There is a fully developed turbulent flow.
- $T_\nu \approx T_t$ i.e. $\mathrm{Re}_l \approx 1$: transition state, laminar stationary flow into turbulent and unsteady, if exceeded the critical Reynolds number.

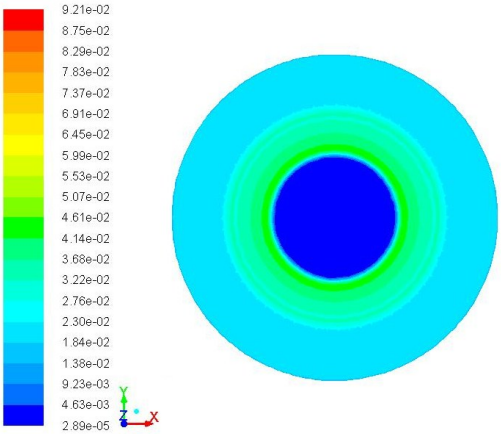

Fig. 3 Cell Reynolds number in axial hydrostatic bearing with circular central groove.

In the Fluent Cell Reynolds Number is defined as

$$\mathrm{Re} = \frac{\rho \cdot u \cdot l}{\mu_{eff}}, \tag{3}$$

where:

u is the velocity magnitude,

μ_{eff} is the effective viscosity (laminar plus turbulent),

l is the characteristic length calculated from the individual cell volume of the computational grid, i.e. $l = \sqrt{V_{cell}}$ for 2D grid and $l = \sqrt[3]{V_{cell}}$ in 3D or axisymmetric cases.

In Fig. 3 the evaluation of Cell Reynolds number for axial hydrostatic bearing with circular central groove is presented. The value of Cell Reynolds number is much smaller than 1, ranging from 2.89 10^{-5} to 9.21 10^{-2}. Laminar flow can be assumed in the narrow gap of the bearing.

3 EVALUATION OF THE MATHEMATICAL MODEL OF THE AXIAL HYDROSTATIC BEARING WITH CENTRAL GROOVE

To evaluate the flow field parameters, graphical output was created on evaluation plain, which is located in the middle of the gap thickness. In this plane the pressure field for the depth of grooves 2 mm was depicted, see Fig. 4. We can compare all three variants. For variant a) the static pressure reaches its maximum in a circular grease pocket. Its value is approximately 7 MPa. Then the pressure drops to zero (atmospheric pressure) at the outflow from the bearing, where there is the atmospheric pressure. Descent is parabolic course.

Tab. 1 Load capacity of the axial hydrostatic bearing with central groove.

Variant	Load capacity [N]	
	Depth of groove 2 mm	Depth of groove 0.2 mm
a)	624763.4	382492.7
b)	262682.7	275803.1
c)	269764.1	308473.7

For variant b) and c) we can see how the liquid is distributed by grooves. Maximum static pressure is approximately 2.2 MPa. This large decrease is attributable to influence of the groove profile. As the groove depth is 2 mm and fluid layer 0.13 mm, almost all the fluid flows through the pockets. This causes the faster drainage of the oil from the bearing.

In Tab. 1 we can see the load capacity of individual variants. Variant a) has the greatest load capacity. Load capacity of variants b) and c) are approximately the same. Load capacity was evaluated on the upper plate using Ansys Fluent software. The total force component along the specified force vector on a wall zone is computed by summing the dot product of the pressure and viscous forces on each face with the specified force vector [8]:

$$F_{\mathbf{a}} = \mathbf{a} \cdot \mathbf{F}_p + \mathbf{a} \cdot \mathbf{F}_v \tag{4}$$

where:

a is a specified force vector,

$\mathbf{F}_p$ is a pressure force vector,

$\mathbf{F}_v$ is a viscous force vector.

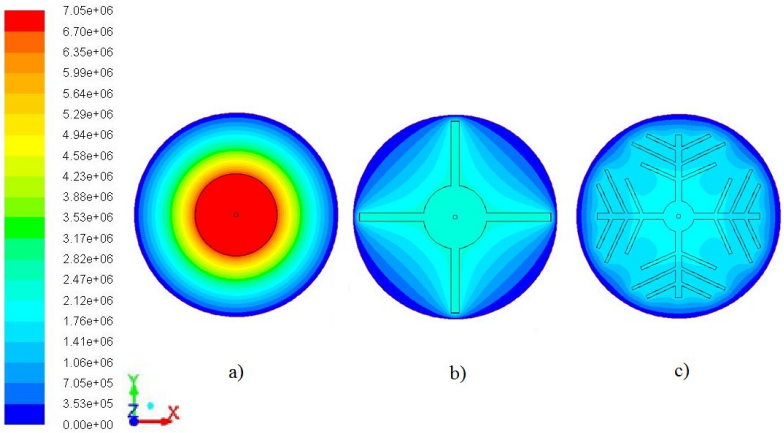

Fig. 4 Pressure field in the axial hydrostatic bearing with central groove, depth of groove 2 mm, unit [Pa].

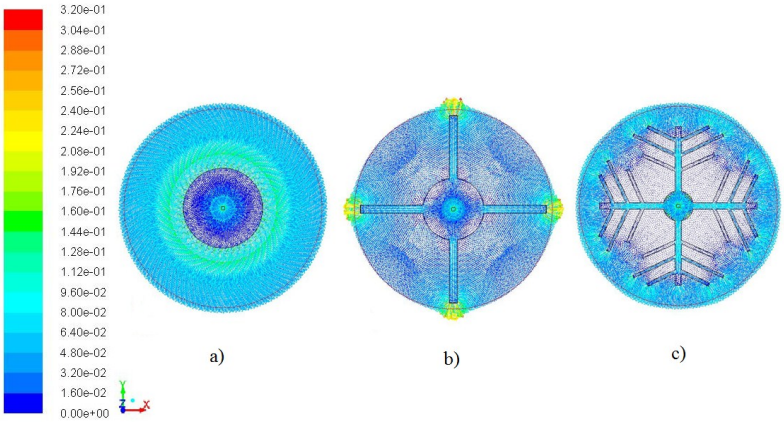

Fig. 5 Velocity vectors in the axial hydrostatic bearing with central groove, depth of groove 2 mm, unit [m.s^{-1}].

Fig. 5 shows velocity vectors of the axial hydrostatic bearings with central grooves for depth of grooves 2 mm. For variant a) speed is not affected by the grooves, so the fluid flows in all directions evenly. Maximum speed is in the fluidized layer after leaving the pocket, because it significantly reduces the cross section of the flowing oil. For variant b) and c) we can see that a large part of the liquid is carried out of grooves. The fluid can flow in all directions, and chooses the path of least resistance.

Since mineral oil is rapidly leaded away from the bearing, the depth of oil groove was adjusted to 0.2 mm. When comparing the pressure fields in the axial hydrostatic bearings, it has been found that the depth reduction has a significant influence on pressure distribution. For variant a) is the maximum static pressure only at the entrance to the bearing and already in a circular pocket it gradually decreases. This is in contrast with the deeper groove bearings, where the same value of maximum static pressure can be observed across the whole circular groove. For variant b) and c) static pressure is increased at the point of entry. It is no longer as evenly spread as in the case of deeper grooves. This is probably due to the fact that the liquid is no longer so quickly drained from the bearing. Figure 7 shows velocity vectors of the axial hydrostatic bearings with central grooves for depth of grooves 0.2 mm. In tab. 1 load capacity of the axial hydrostatic bearing is compared for both values of the groove depth. For variant a) the load capacity decreased with groove depth reduction almost by half. In contrast in the variant b) the load capacity increases by 13000 N and for variant c) by 38000 N.

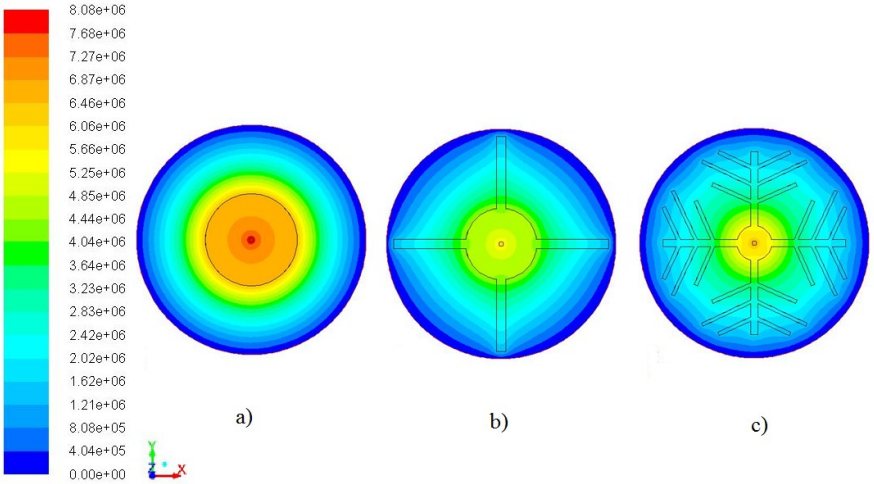

Fig. 6 Pressure field in the axial hydrostatic bearing with central groove, depth of groove 0.2 mm, unit [Pa].

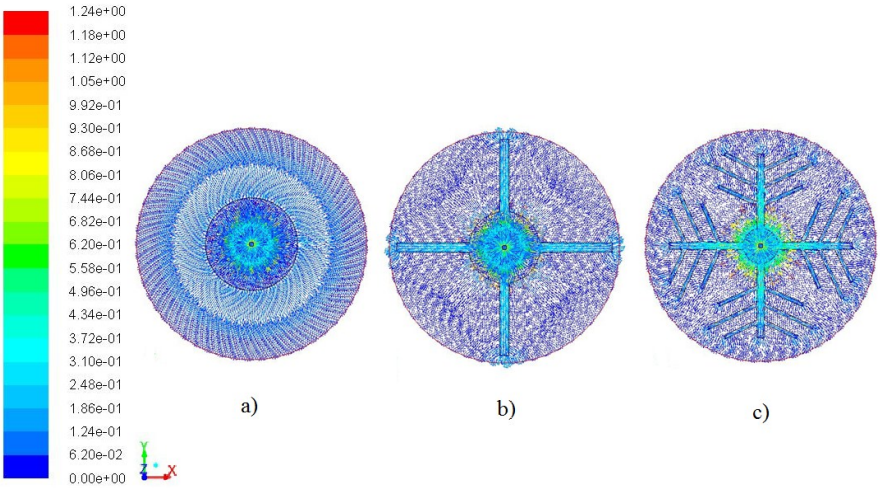

Fig. 7 Velocity vectors in the axial hydrostatic bearing with central groove, depth of groove 0.2 mm, unit [$m.s^{-1}$].

4 CONCLUSIONS

In the article three variants of lubrication grooves are compared. Pressure field, velocity vectors and load capacity were evaluated and compared. In addition, the influence of oil groove depth was investigated.

Variant a) has the greatest load capacity, but can be loaded only in the axis of rotation. It can be concluded that with increasing groove depth the load capacity of the bearing increases.

For variant b) an c) on the contrary, can be stated that with increasing groove depth the load capacity of the bearing is decreasing. From these two variants c) seems to be better. The mineral oil is rapidly distributed over the bearing by radial grooves and oblique grooves cause an even distribution of pressure over the entire area. This allows loading the bearing by eccentric forces.

REFERENCES

[1] WECK, M.; HENNING, J.; WINTERSCHLADEN, M.: *Development of hydrostatic bearings with groove structures. Initiatives of precision engineering at the beginning of a milennium.* Yokohama. 2011. ISBN 0-306-47000-4

[2] NIEWSTADT, F.T.M. et al.: *Direct and Large Eddy simulations of turbulence in fluids*. Future Generation Computer System, 1994, p.189-205.

[3] KOZDERA, M: *Projekční návrhy axiálních hydrostatických ložisek.* Diplomová práce, Ostrava, VŠB – TU Ostrava, 2010

[4] KOZUBKOVÁ, M: *Modelování proudění – Fluent*. Ostrava, VŠB – TU Ostrava, 2008, 142 s.

[5] BEČKA, J.: *Tribologie*. Praha, 1997, 212 s. ISBN 80-01-01621-8

[6] VINŠ, J.: *Kluzná ložiska*. Praha, 1971, 376 s. ISBN 04-235-71

[7] BLAŠKOVIČ, P.; BALLA J.; DZIMKO M.: *Tribológia*. Bratislava, 1990, 360 s. ISBN 80-05-00633-0

[8] FLUENT 6.3.26 – *User´s guide*. Fluent Inc. 2003 [online]. Datum poslední revize 3.10.2006 [cit. 2008-12-08]. Dostupné z < http://spc.vsb.cz/ >.

The results presented in this paper were achieved within the specific research project SP2012/55 “Modelování dynamiky tekutinových mechanismů” solved at Faculty of Mechanical Engineering, VŠB – Technical University of Ostrava in 2012.